

**Metal Germlyne Complexes [M≡Ge–R] and
Metallogermlynes [M–Ge–R]: DFT Analysis of the Systems
[(Cp)(CO)_nM≡GeMe] (M = Cr, Mo, W, Fe²⁺, n = 2; M = Fe,
n = 1) and [(Cp)(CO)_nM–GeMe] (M = Cr, Mo, W, n = 3; M =
Fe, n = 2)**

Krishna K. Pandey,^{*,†,‡} Matthias Lein,[‡] and Gernot Frenking^{*,‡}

*Contribution from the School of Chemical Sciences, Devi Ahilya University Indore,
Indore, India 452017, and Fachbereich Chemie, Philipps-Universität Marburg,
D-35037 Marburg, Germany*

Received July 16, 2002; Revised Manuscript Received November 27, 2002 E-mail: frenking@chemie.uni-marburg.de

Abstract: Quantum chemical calculations at the gradient corrected DFT level using the exchange correlation functionals BP86 and B3LYP of the geometries of the title compounds are reported. The theoretically predicted bond lengths and angles of the model compounds are in excellent agreement with experiment. The nature of the metal–ligand interactions is quantitatively analyzed with an energy decomposition method. The analysis of the electronic structure of the neutral metal germlyne complexes **1a–1d** and the metallogermlynes **11a–11d** shows that the former compounds have about the same degree of electrostatic and covalent bonding, while the relative strength of the covalent contributions in the latter molecules is lower (41–42%) than the electrostatic attraction (58–59%). The $\sigma(\pi)$ bonding contribution in the group-6 germlyne complexes **1a–1c** is rather high (42% of the orbital interactions). In the iron complex **1d**, it is even higher (53.8%) than the σ bonding. The π bonding contributions to the covalent bonding become much less (18–20%) in the metallogermlynes **11a–11d**.

Introduction

The chemistry of transition metal carbyne complexes has been the focus of intensive experimental and theoretical work in recent years.^{1–8} Thirty years after the first synthesis of a metal-carbyne complex⁹ and twenty-eight years after the isolation of the first metallocarbonyl complex,¹⁰ it can be stated that much knowledge about the properties of the molecules has been gained. In sharp contrast to complexes with carbyne ligands CR, the research about heavier analogues with ligands ER (E = Si, Ge, Sn, Pb) has been scarce, and attempts to synthesize the latter compounds were much less successful. In fact, transition metal silylyne,¹¹ stannylyne, and plumblylyne complexes are presently unknown, and it is remarkable that only a few transition metal germlyne complexes could become

isolated so far.^{12–15} Chart 1 gives an overview of some germlyne complexes **1–10** that have been reported in the literature.

A characteristic feature of the compounds **1–10** is that the M–Ge–R linkage is linear. Thus, the bonding situation in the molecules can be explained with the same model that is used for carbyne complexes (Figure 1a).^{5,6} The model considers a formally positively charged ligand GeR⁺, which serves as a two-electron σ donor and a four-electron π acceptor. The π interactions in molecules which have only C_s symmetry are then labeled as in-plane (π_{\parallel}) and out-of-plane (π_{\perp}) π contributions. The germlyne complexes **1–10** are thus 18-electron complexes.

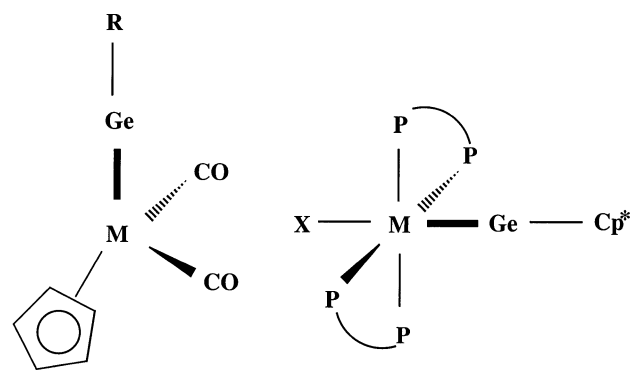
Very recently, complexes [M]GeR, which have a strongly bent M–Ge–R linkage (Chart 2), were synthesized and structurally characterized. The bond angles in **11** and **12** are between 114.7° and 117.8°. The geometries, molecular composition, and chemical properties of the molecules suggest that the M–GeR bonding situation is significantly different from the bonding situation in molecules **1–10**.

[†] Devi Ahilya University Indore.

[‡] Philipps-Universität Marburg.

- (1) Nugent, W. A.; Mayer, J. M. *Metal–Ligand Multiple Bonds*; Wiley: New York, 1988.
- (2) Fischer, H.; Hofmann, P.; Kreisal, F. R.; Schrock, R. R.; Schubert, U.; Weiss, K. *Carbyne Complexes*; VCH: New York, 1988.
- (3) *Transition Metal Carbyne Complexes*; Kreisel, F. R., Ed.; Kluwer: Dordrecht, The Netherlands, 1993.
- (4) LaPoint, A. M.; Schrock, R. R.; Davis, W. M. *J. Am. Chem. Soc.* **1995**, *117*, 4802.
- (5) Vyboishchikov, S. F.; Frenking, G. *Chem.-Eur. J.* **1998**, *4*, 1439.
- (6) Frenking, G.; Fröhlich, N. *Chem. Rev.* **2000**, *100*, 717.
- (7) Cho, S. K.; Gal, Y. S.; Jin, S. H.; Kim, H. K. *Chem. Rev.* **2000**, *100*, 1645.
- (8) Herndon, J. W. *Coord. Chem. Rev.* **2002**, *227*, 1.
- (9) Fischer, E. O.; Kreis, G.; Kreiter, C. G.; Müller, J.; Huttner, G.; Lorenz, H. *Angew. Chem., Int. Ed. Engl.* **1973**, *12*, 564.
- (10) McLain, S. J.; Wood, C. D.; Messerle, L. W.; Schrock, R. R.; Hollander, F. J.; Youngs, W. J.; Churchill, M. R. *J. Am. Chem. Soc.* **1978**, *100*, 5962.

- (11) The previously reported complex [η^5 -C₅Me₅](Me₃P)₂RuSi{(bipy)(SC₆H₄-4-Me)}][OTf]₂ can be formally described as a silylyne complex which has four coordinated silicon. Grumbine, S. D.; Chadha, R. K.; Tilley, T. D. *J. Am. Chem. Soc.* **1992**, *114*, 1518.
- (12) Simons, R. S.; Power, P. P. *J. Am. Chem. Soc.* **1996**, *118*, 11966.
- (13) Pu, L.; Twamley, B.; Haubrich, S. T.; Olmstead, M. M.; Mork, B. V.; Simons, R. S.; Power, P. P. *J. Am. Chem. Soc.* **2000**, *122*, 650.
- (14) Filippou, A. C.; Philippopoulos, A. I.; Portius, P.; Neumann, D. U. *Angew. Chem., Int. Ed.* **2000**, *39*, 2778.
- (15) Filippou, A. C.; Portius, P.; Philippopoulos, A. I. *Organometallics* **2002**, *21*, 653.

Chart 1. Overview of Experimentally Known Metal Germylyne Complexes

R	M	X	No
$C_6H_3-2,6-(C_6H_2-2,4,6-iPr_3)_2$	Cr		1
$C_6H_3-2,6-(C_6H_2-2,4,6-iPr_3)_2$	Mo		2
$C_6H_3-2,6-(C_6H_2-2,4,6-iPr_3)_2$	W		3
$C_6H_3-2,6-(C_6H_2-2,4,6-Me_3)_2$	Mo		4
$C_6H_3-2,6-(C_6H_2-2,4,6-Me_3)_2$	W		5
P-P= dppe, Cp* = C_5Me_5	Mo	Cl	6
P-P= dppe, Cp* = C_5Me_5	Mo	Br	7
P-P= dppe, Cp* = C_5Me_5	W	Cl	8
P-P= dppe, Cp* = C_5Me_5	W	Br	9
P-P= dppe, Cp* = C_5Me_5	W	I	10

A comparison of compounds **11** and **12** (Chart 2) with **1** and **3** (Chart 1) shows that the former compounds have one more CO ligand than the latter. The 18-electron rule suggests that the (formally) positively charged germylyne ligand GeR^+ in **11** and **12** cannot serve as a two-electron donor like in **1** and **3**, because the metal fragment of the former species has two more electrons. The d_z^2 acceptor orbital of the metal is occupied, and thus it cannot serve as a σ acceptor orbital (Figure 1b). The other d-orbitals of the metal cannot serve as acceptor orbitals because the interaction is symmetry forbidden. Attractive orbital interactions between GeR^+ and the metal fragment of **11–15** are only possible when the germylyne ligand is bonded in a side-on fashion (Figure 1c). The qualitative bonding model in Figure 1c shows that the M–GeR bonding has two components, that is, σ donation from the occupied metal d_{z^2} and d_{yz} orbitals into the in-plane $p(\pi)$ atomic orbital (AO) of Ge and π_{\perp} donation from the occupied metal d_{xz} orbital into the out-of-plane $p(\pi)$ AO of Ge. The former interactions should lead to some rehybridization (see Figure 1c), which will be discussed below. It follows that compounds **11–15** should rather be considered as derivatives of germylenes GeR_2 ; that is, they are *metallogermylenes* $[M]-Ge-R$ and not germylyne complexes $[M]\equiv GeR$. It is worth pointing out that the related *metallocarbenes* are still unknown. This is probably related to the known instability of carbenes. Because N-heterocyclic carbenes (Arduengo carbenes) are stable compounds,¹⁶ it seems feasible that related metallo-carbenes could become isolated.

(16) (a) Arduengo, A. J.; Harlow, R. L.; Kline, M. J. *Am. Chem. Soc.* **1991**, *113*, 361. (b) Arduengo, A. J. *Acc. Chem. Res.* **1999**, *32*, 913.

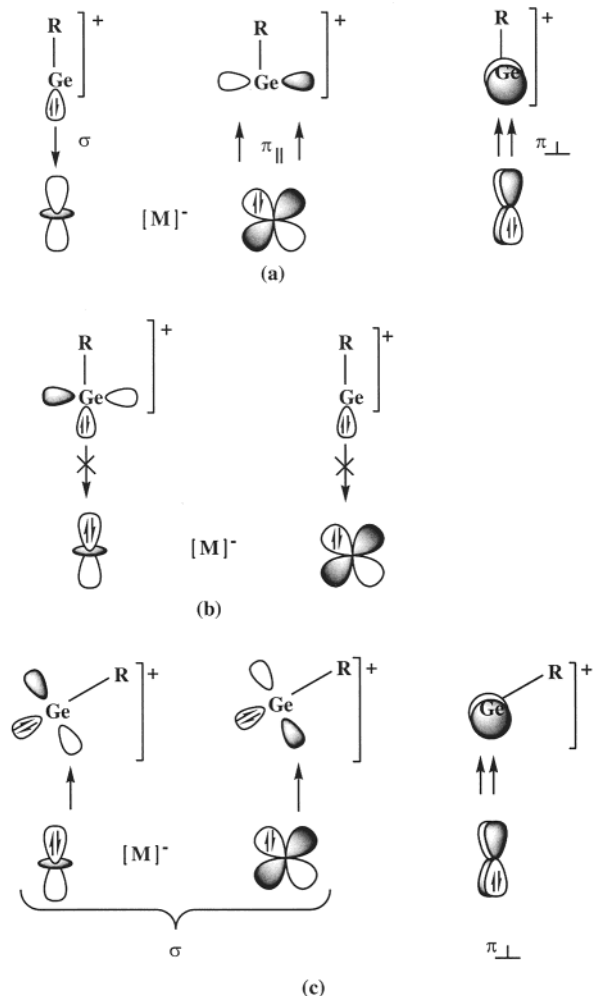
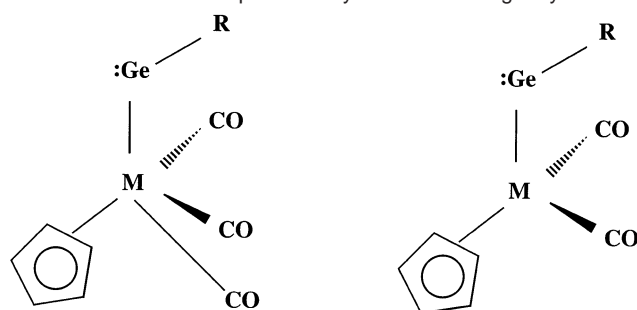


Figure 1. Schematic representation of the orbital interactions between closed-shell metal fragments $[M]^-$ and germylyne ligands GeR^+ in (a) metal germylyne complexes with 16-electron fragments $[M]^-$; (b) metal germylyne complexes with 18-electron fragments $[M]^-$; and (c) metallogermylenes.

In recent years, there has been considerable interest in the investigation of the synthesis, structure, bonding, and reactivities of monomeric germylenes.^{17–24} For the known σ bonded monomeric alkyl or aryl germylenes,^{25–30} the Ge–C bond lengths range between 1.80 and 2.08 Å, and the C–Ge–C bond angle varies from 85.9 to 111.4°. The contraction of the bond angle and the simultaneous lengthening of the Ge–C bond are consistent with a decreased s-character of the Ge–C bond.³¹ Jutzi and Leue³² isolated the first metallogermylene derivatives

- (17) Petz, W. *Chem. Rev.* **1986**, *86*, 1019.
 (18) Barrau, J.; Escudie, J.; Satge, J. *Chem. Rev.* **1990**, *90*, 283.
 (19) Neumann, W. P. *Chem. Rev.* **1991**, *91*, 311.
 (20) Lappert, M. F.; Rowe, R. S. *Coord. Chem. Rev.* **1990**, *100*, 267.
 (21) Jutzi, P. *Adv. Organomet. Chem.* **1986**, *26*, 258.
 (22) Driess, M.; Grützmacher, H. *Angew. Chem., Int. Ed. Engl.* **1996**, *35*, 828.
 (23) Lappert, M. F. *Main Group Met.* **1994**, *17*, 183.
 (24) Barrau, J.; Rima, G. *Coord. Chem. Rev.* **1998**, *178–180*, 593.
 (25) Davidson, P. J.; Harris, D. H.; Lappert, M. F. *J. Chem. Soc., Dalton Trans.* **1976**, 2268.
 (26) Fjeldberg, T.; Haaland, A.; Schilling, B. E. R.; Lappert, M. F.; Thorne, A. J. *J. Chem. Soc., Dalton Trans.* **1986**, 1551.
 (27) Jutzi, P.; Becker, A.; Stammler, H. G.; Neumann, B. *Organometallics* **1991**, *10*, 1647.
 (28) Jutzi, P.; Schmidt, H.; Neumann, B.; Stammler, H. G. *Organometallics* **1996**, *15*, 741.
 (29) Tokitoh, N.; Manmaru, K.; Okazaki, R. *Organometallics* **1994**, *13*, 167.
 (30) Bender, J. E.; Holl, M. M. B.; Kampf, J. W. *Organometallics* **1997**, *16*, 22743.
 (31) Grev, R. S.; Schaefer, H. F., III. *Organometallics* **1992**, *11*, 3489.
 (32) Jutzi, P.; Leue, C. *Organometallics* **1994**, *13*, 2898.

Chart 2. Overview of Experimentally Known Metallogermynes



R	(CO) _n	M	No
C ₆ H ₃ -2,6-(C ₆ H ₂ -2,4,6-iPr ₃) ₂	n = 3	Cr	11
C ₆ H ₃ -2,6-(C ₆ H ₂ -2,4,6-iPr ₃) ₂	n = 3	W	12
CH(SiMe ₃) ₂	n = 2	Fe	13
C ₆ H ₂ -2,4,6-(tBu ₃) ₃	n = 2	Fe	14
C ₆ H ₂ -2,4,6-(tBu ₃) ₃	n = 2	Fe	15 (Cp⁺)

of iron, but no structures have been determined. In 2000, Power et al. reported the first structurally characterized metallogermynes **11** and **12** (Chart 2).¹³

The electronic structure and bonding situation of carbyne complexes have been investigated in several theoretical studies,^{2,5,6} but very little attention has been paid to germylene complexes. In a recent communication, a density functional analysis of model tungsten-germylene complexes [Cl(L)₄W≡Ge(η¹-C₅H₅)] (L = CO, PH₃) has been reported, but a bond decomposition analysis which provides insight into the nature of the bond was not given.¹⁴ The differences between the bonding situation of germylene complexes which have a linear M–Ge–R linkage with metallogermynes have never been studied before. We decided to investigate the chemical bonding in the two classes of compound with an energy decomposition analysis. It has been shown that the results give a quantitative insight into the nature of the metal–ligand interactions.³³

In this paper, five metal germylene complexes, [(η⁵-C₅H₅)(CO)₂M≡GeMe] (**Ia**, M = Cr; **Ib**, M = Mo; **Ic**, M = W), [(η⁵-C₅H₅)(CO)Fe≡GeMe], **Id**, [(η⁵-C₅H₅)(CO)₂Fe≡GeMe]²⁺, **Ie**, and four metallogermynes [M–GeMe], that is, [(η⁵-C₅H₅)(CO)₃M–GeMe] (**IIa**, M = Cr; **IIb**, M = Mo; **IIc**, M = W) and [(η⁵-C₅H₅)(CO)₂Fe–GeMe], **IId**, have been investigated at the DFT level using B3LYP and BP86. The compounds **Ia–Ic** serve as models for **1–10**, while **IIa–IId** are models for **11–15**. In the model complexes, the bulky substituents at germanium atom are replaced by a methyl group. The choice of the model compounds was made with the goal to compare (a) the differences between the germylene complexes **Ia–Ic** and the metallogermynes **IIa–IIc** of group-6 elements Cr, Mo, W, (b) the differences between the group-6 compounds **Ia** and **IIa** and the group-8 species **Id** and **IId**, and (c) the differences between neutral and charged germylene complexes **Id** and **Ie**.

(33) (a) Diefenbach, A.; Bickelhaupt, F. M.; Frenking, G. *J. Am. Chem. Soc.* **2000**, *122*, 6449. (b) Uddin, J.; Frenking, G. *J. Am. Chem. Soc.* **2001**, *123*, 1683. (c) Frenking, G.; Wichmann, K.; Fröhlich, N.; Loschen, C.; Lein, M.; Frunzke, J.; Rayón, V. M. *Coord. Chem. Rev.*, in print.

The main goals of the present study are (i) to investigate the structures and to analyze the nature of the M–Ge bonds of the germylene complexes and metallogermynes, and (ii) to provide a quantitative differentiation of the bonding between the linear (M≡Ge–R) and the bent (M–Ge–R) coordination modes. This study reports for the first time a comparative theoretical investigation of metallogermynes and metal germylene complexes.

Methods

The calculations were performed at the nonlocal DFT level of theory using the exchange functional of Becke³⁴ and the correlation functional of Perdew³⁵ (BP86). Scalar relativistic effects have been considered using the ZORA formalism.³⁶ Uncontracted Slater-type orbitals (STOs) were used as basis functions for the SCF calculations.³⁷ Triple-ζ basis sets augmented by two sets of polarization functions have been used for all of the elements. The (n – 1)s² and (n – 1)p⁶ core electrons of the main group elements, (1s2s2p)¹⁰ core electrons of chromium and iron, (1s2s2p3s3p3d)²⁸ core electrons of molybdenum, and (1s2s2p3s3p3d4s4p4d)⁴⁶ core electrons of tungsten were treated by the frozen-core approximation.³⁸ An auxiliary set of s, p, d, f, and g STOs was used to fit the molecular densities and to present the Coulomb and exchange potentials accurately in each SCF cycle.³⁹ The calculations were carried out using the program package ADF-2002.01.⁴⁰

Calculations were also performed using the hybrid B3LYP density functional method, which uses Becke's 3-parameter nonlocal exchange functional⁴¹ mixed with the exact (Hartree–Fock) exchange functional and Lee–Yang–Parr's nonlocal correlation functional.⁴² The geometries of all complexes were optimized using C_s symmetry constraints with

(34) Becke, A. D. *J. Chem. Phys.* **1988**, *38*, 3098.

(35) Perdew, J. P. *Phys. Rev. B* **1986**, *33*, 8822.

(36) (a) Chang, C.; Pellissier, M.; Durand, Ph. *Phys. Scr.* **1986**, *34*, 394. (b) Heully, J.-L.; Lindgren, I.; Lindroth, E.; Lundquist, S.; Martensson-Pendrill, A.-M. *J. Phys. B* **1986**, *19*, 2799. (c) van Lenthe, E.; Baerends, E. J.; Snijders, J. G. *J. Chem. Phys.* **1993**, *99*, 4597. (d) van Lenthe, E.; Baerends, E. J.; Snijders, J. G. *J. Chem. Phys.* **1996**, *105*, 6505. (e) van Lenthe, E.; van Leeuwen, R.; Baerends, E. J.; Snijders, J. G. *Int. J. Quantum Chem.* **1996**, *57*, 281. (f) van Lenthe, E.; Ehlers, A. E.; Baerends, E. J. *J. Chem. Phys.* **1999**, *110*, 8943.

(37) Snijders, J. G.; Baerends, E. J.; Vernooijs, P. *At. Data Nucl. Data Tables* **1982**, *26*, 483.

(38) Baerends, E. J.; Ellis, D. E.; Ros, P. *Chem. Phys.* **1973**, *2*, 41.

(39) Krijn, J.; Baerends, E. J. *Fit Functions in the HFS-Method, Internal Report (in Dutch)*; Vrije Universiteit Amsterdam: The Netherlands, 1984.

(40) Baerends, E. J.; Autschbach, J. A.; Berces, A.; Bo, C.; Boerrigter, P. M.; Cavallo, L.; Chong, D. P.; Deng, L.; Dickson, R. M.; Ellis, D. E.; Fan, L.; Fischer, T. H.; Fonseca Guerra, C.; van Gisbergen, S. J. A.; Groeneveld, J. A.; Gritsenko, O. V.; Grüning, M.; Harris, F. E.; van den Hoek, P.; Jacobsen, H.; van Kessel, G.; Kootstra, F.; van Lenthe, E.; Osinga, V. P.; Patchkovskii, S.; Philipsen, P. H. T.; Post, D.; Pye, C. C.; Ravenek, W.; Ros, P.; Schipper, P. R. T.; Schreckenbach, G.; Snijders, J. G.; Sola, M.; Swart, M.; Swerhone, D.; te Velde, G.; Vernooijs, P.; Versluis, L.; Visser, O.; Wezenbeek, E.; Wiesenecker, G.; Wolff, S. K.; Woo, T. K.; Ziegler, T. *ADF 2002-01*; Scientific Computing & Modelling NV: The Netherlands.

(41) Becke, A. D. *J. Chem. Phys.* **1993**, *98*, 5648.

(42) Lee, C.; Yang, W.; Parr, R. G. *Phys. Rev. B* **1988**, *17*, 785.

(43) (a) Krishnan, R.; Binkley, J. S.; Seeger, R.; Pople, J. A. *J. Chem. Phys.* **1980**, *72*, 650. (b) McClean, A. D.; Chandler, G. S. *J. Chem. Phys.* **1980**, *72*, 5639.

(44) (a) Hay, P. J.; Wadt, W. R. *J. Chem. Phys.* **1985**, *82*, 270. (b) Wadt, W. R.; Hay, P. J. *J. Chem. Phys.* **1985**, *82*, 284. (c) Hay, P. J.; Wadt, W. R. *J. Chem. Phys.* **1985**, *82*, 299.

(45) Reed, A. E.; Curtiss, L. A.; Weinhold, F. *Chem. Rev.* **1988**, *88*, 899.

(46) Frisch, M. J.; Trucks, G. W.; Schlegel, H. B.; Scuseria, G. E.; Robb, M. A.; Cheeseman, J. R.; Zakrzewski, V. G.; Montgomery, J. A., Jr.; Stratmann, R. E.; Burant, J. C.; Dapprich, S.; Millam, J. M.; Daniels, A. D.; Kudin, K. N.; Strain, M. C.; Farkas, O.; Tomasi, J.; Barone, V.; Cossi, M.; Cammi, R.; Mennucci, B.; Pomelli, C.; Adamo, C.; Clifford, S.; Ochterski, J.; Petersson, G. A.; Ayala, P. Y.; Cui, Q.; Morokuma, K.; Salvador, P.; Dannenberg, J. J.; Malick, D. K.; Rabuck, A. D.; Raghavachari, K.; Foresman, J. B.; Cioslowski, J.; Ortiz, J. V.; Baboul, A. G.; Stefanov, B. B.; Liu, G.; Liashenko, A.; Piskorz, P.; Komaromi, I.; Gomperts, R.; Martin, R. L.; Fox, D. J.; Keith, T.; Al-Laham, M. A.; Peng, C. Y.; Nanayakkara, A.; Challacombe, M.; Gill, P. M. W.; Johnson, B.; Chen, W.; Wong, M. W.; Andres, J. L.; Gonzalez, C.; Head-Gordon, M.; Replogle, E. S.; Pople, J. A. *Gaussian 98*, revision A.11; Gaussian, Inc.: Pittsburgh, PA, 2001.

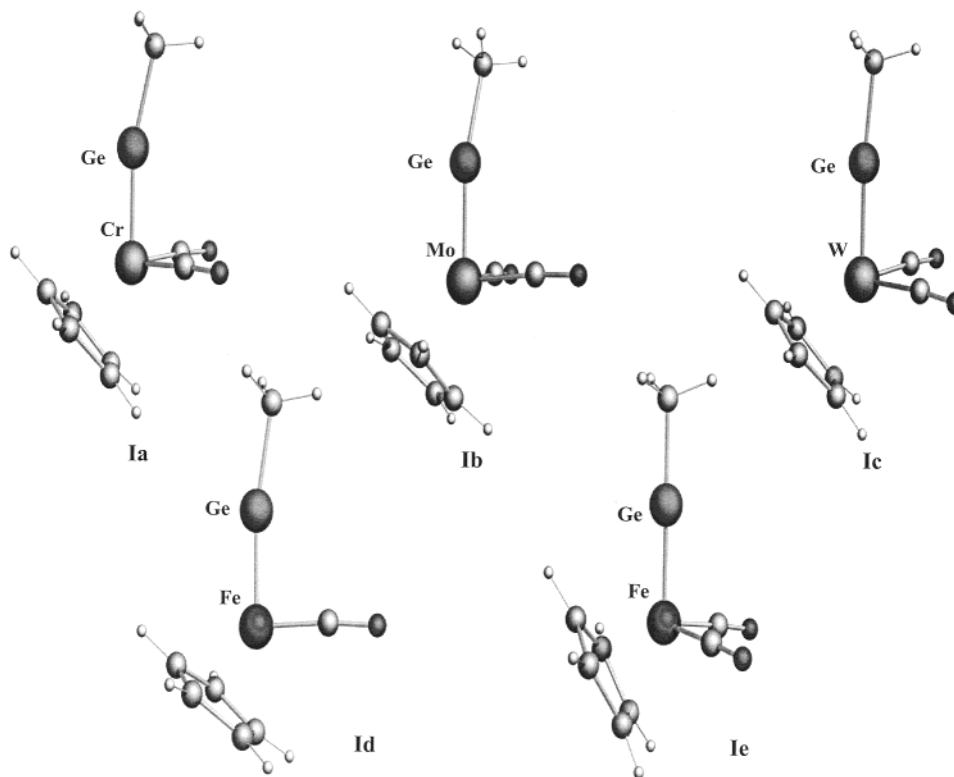


Figure 2. Optimized geometries of the metal germlyne complexes **Ia–Ie**. The most important bond lengths and angles are given in Table 1.

standard 6-311G(d) basis sets⁴³ for Cr, Fe, Ge, O, C, and H elements and LANL2DZ⁴⁴ for Mo and W which combines quasi-relativistic effective core potentials with a valence double- ζ basis set. Frequency calculations were performed to determine whether the optimized geometries were minima on the potential energy surface. The electronic structure of the complexes was examined by NBO analysis.⁴⁵ The latter calculations were carried out with the Gaussian 98 program.⁴⁶

The bonding interactions between the metal fragments $[(\eta^5\text{-C}_5\text{H}_5)(\text{CO})_2\text{M}]^-$, $[(\eta^5\text{-C}_5\text{H}_5)(\text{CO})_3\text{M}]^-$ ($\text{M} = \text{Cr}, \text{Mo}, \text{W}$), $[(\eta^5\text{-C}_5\text{H}_5)(\text{CO})\text{-Fe}]^-$, $[(\eta^5\text{-C}_5\text{H}_5)(\text{CO})_2\text{Fe}]^+$, $[(\eta^5\text{-C}_5\text{H}_5)(\text{CO})_2\text{Fe}]^-$, and the ligand GeMe^+ have been analyzed using the energy decomposition scheme of ADF, which is based on the methods of Morokuma⁴⁷ and Ziegler and Rauk.⁴⁸ The bond dissociation energy ΔE between two fragments A and B is partitioned into several contributions that can be identified as physically meaningful entities. First, ΔE is separated into two major components ΔE_{prep} and ΔE_{int} :

$$\Delta E = \Delta E_{\text{prep}} + \Delta E_{\text{int}} \quad (1)$$

Here, ΔE_{prep} is the energy that is necessary to promote the fragments A and B from their equilibrium geometry and electronic ground state to the geometry and electronic state that they have in the compound AB. ΔE_{int} is the interaction energy between the two fragments in the molecule. The interaction energy, ΔE_{int} , can be divided into three main components:

$$\Delta E_{\text{int}} = \Delta E_{\text{elstat}} + \Delta E_{\text{Pauli}} + \Delta E_{\text{orb}} \quad (2)$$

ΔE_{elstat} gives the electrostatic interaction energy between the fragments that is calculated using the frozen electron density distribution of A and B in the geometry of the complex AB. The second term in eq

2, ΔE_{Pauli} , gives the repulsive interactions between the fragments that are due to the fact that two electrons with the same spin cannot occupy the same region in space. The term comprises the four-electron destabilizing interactions between occupied orbitals. ΔE_{Pauli} is calculated by enforcing the Kohn–Sham determinant of AB, which results from superimposing fragments A and B, to obey the Pauli principle through antisymmetrization and renormalization. The stabilizing orbital interaction term ΔE_{orb} is calculated in the final step of the energy analysis when the Kohn–Sham orbitals relax to their optimal form. The latter term can be further partitioned into contributions by the orbitals that belong to different irreducible representations of the point group of the system. The covalent and electrostatic character of the bond is given by the ratio $\Delta E_{\text{elstat}}/\Delta E_{\text{orb}}$.³³

Geometries

Metal-Germlyne Complexes $[(\eta^5\text{-C}_5\text{H}_5)(\text{CO})_2\text{M}\equiv\text{GeMe}]$ (Ia**, $\text{M} = \text{Cr}$; **Ib**, $\text{M} = \text{Mo}$; **Ic**, $\text{M} = \text{W}$), $[(\eta^5\text{-C}_5\text{H}_5)(\text{CO})\text{-Fe}\equiv\text{GeMe}]$, **Id**, and $[(\eta^5\text{-C}_5\text{H}_5)(\text{CO})_2\text{Fe}\equiv\text{GeMe}]^{2+}$, **Ie**.** Figure 2 shows the optimized geometries of the metal germlyne complexes **Ia–Ie**. The optimized bond lengths and angles at B3LYP and BP86 are presented in Table 1. The structures of the chromium, molybdenum, and tungsten model germlyne complexes closely resemble those found by X-ray diffraction for **1**, **2**, **4**, and **5**.^{12,13} The B3LYP and BP86 values are very similar to each other. The calculated bond lengths at BP86 are in slightly better agreement with the experimental values than are the B3LYP values. On going from chromium to tungsten, we observe a steady increase of the M–Ge bond distance from 2.156 (**Ia**) to 2.286 (**Ib**) to 2.293 Å (**Ic**). The neutral iron complex, **Id**, has an Fe–Ge distance of 2.091 Å, which is the shortest metal–germylyne bond distance of the complexes investigated in this study. The cationic iron complex, **Ie**, which is isosteric and isoelectronic to the complexes of the chromium triad, has an Fe–Ge distance of 2.149 Å at BP86. The M–Ge

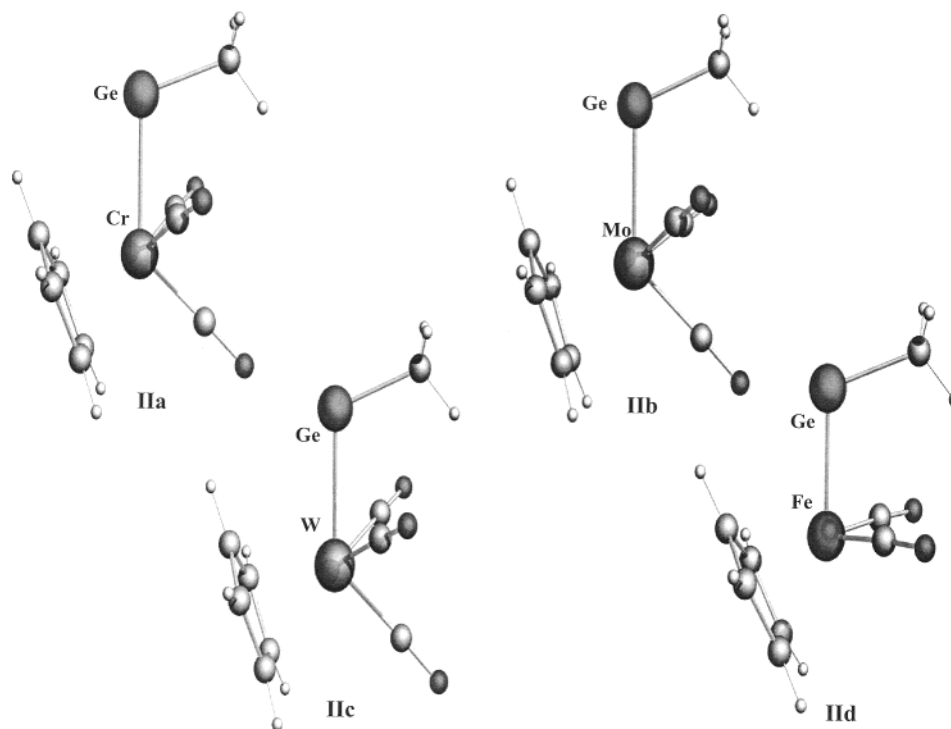
(47) (a) Morokuma, K. *J. Chem. Phys.* **1971**, *55*, 1236. (b) Morokuma, K. *Acc. Chem. Res.* **1977**, *10*, 294.

(48) (a) Ziegler, T.; Rauk, A. *Theor. Chim. Acta* **1977**, *46*, 1. (b) Ziegler, T.; Rauk, A. *Inorg. Chem.* **1979**, *18*, 1558. (c) Ziegler, T.; Rauk, A. *Inorg. Chem.* **1979**, *18*, 1755.

Table 1. Selected Optimized Geometrical Parameters for Metal Germylene Complexes $[(\eta^5\text{-C}_5\text{H}_5)(\text{Co})_2\text{M}\equiv\text{GeMe}]$ (M = Cr, Mo, W), $[(\eta^5\text{-C}_5\text{H}_5)(\text{CO})\text{Fe}\equiv\text{GeMe}]$, and $[(\eta^5\text{-C}_5\text{H}_5)(\text{Co})_2\text{Fe}\equiv\text{GeMe}]^{2+}$, and X-ray Data of **1**, **2**, **4**, and **5**^{a,b}

	M = Cr (1a)			M = Mo (1b)				M = W (1c)			M = Fe (1d)		M = Fe ²⁺ (1e)	
	B3LYP	BP86	X-ray (1)	B3LYP	BP86	X-ray (2)	X-ray (4)	B3LYP	BP86	X-ray (5)	B3LYP	BP86	B3LYP	BP86
	Bond Distances													
M–Ge	2.180	2.156	2.1666(4)	2.309	2.286	2.272(8)	2.271(1)	2.312	2.293	2.2767(14)	2.193	2.149	2.094	2.091
M–CO	1.837	1.831	1.850(2)	1.983	1.967	1.959(5)	1.950(9)	1.977	1.971	1.92(2)	1.834	1.811	1.751	1.746
			1.846(2)			1.974(6)	1.960(3)			1.946(15)				
M–C(Cp)av	2.230	2.212	2.190(5)	2.406	2.378	2.335(7)	2.33(3)	2.394	2.371	2.32(2)	2.184	2.141	2.100	2.094
Ge–CH ₃	1.987	1.981	1.9512(18)	1.984	1.979	1.936(5)	1.933(7)	1.978	1.975	1.916(11)	1.915	1.928	1.977	1.982
C–O	1.164	1.171	1.151(6)	1.163	1.170	1.149(9)	1.169(10)	1.166	1.171	1.18(2)	1.135	1.140	1.157	1.174
	Bond Angles													
M–Ge–CH ₃	164.6	165.1	175.99(6)	169.9	166.4	174.25(14)	172.2(2)	174.1	174.4	170.9(3)	178.9	180.0	169.5	169.2
Ge–M–CO	89.6	87.7	89.84(6)	88.8	85.8	91.95(14)	88.2(2)	89.7	88.1	91.8(4)	97.2	95.4	86.7	87.7
			94.28(6)			89.45(16)	86.6(3)			83.1(4)				
C(O)–M–C(O)	92.1	91.6	88.98(9)	90.4	89.5		87.1(2)	90.6	89.9	86.6(6)	92.6	92.9		

^a Distances are in Å, and angles are in degrees. ^b X-ray data are taken from ref 13.

**Figure 3.** Optimized geometries of the metal germylenes **IIa–IIc**. The most important bond lengths and angles are given in Table 2.

bond distances are significantly shorter than those expected for single bonds based on covalent radii predictions (Cr–Ge = 2.50 Å, Mo–Ge = 2.62 Å, W–Ge = 2.63 Å, and Fe–Ge = 2.48 Å).⁴⁹ Using the relationship between bond order and bond distance suggested by Pauling, we find that the calculated M–Ge distances correspond to a bond order of ~ 3 .⁵⁰ A number of complexes featuring Mo–Ge and W–Ge single bonds have been characterized. These include the molybdenum complexes *trans*- $[(\eta^5\text{-C}_5\text{H}_5)\text{Mo}(\text{CO})_2(\text{PMe}_3)(\text{GeCl}_3)]$ ⁵¹ with Mo–Ge = 2.5057(6) Å, *trans*- $[(\eta^5\text{-C}_5\text{H}_5)\text{Mo}(\text{CO})_2(\text{PMe}_3)(\text{GeHCl}_2)]$ ⁵² with

Mo–Ge = 2.531(2) Å, $[(\eta^5\text{-C}_5\text{H}_5)\text{Mo}(\text{CO})_3(\text{GeCl}_3)]$ with Mo–Ge = 2.546(1) Å,⁵¹ $[(\eta^5\text{-C}_5\text{H}_5)\text{Mo}(\eta^3\text{-C}_6\text{H}_{11})(\text{NO})(\text{GePh}_3)]$ with Mo–Ge = 2.604(2) Å,⁵³ $[(\eta^5\text{-C}_5\text{H}_5)\text{Mo}(\text{CO})_2\{\text{C}(\text{OEt})\text{Ph}\}(\text{GePh}_3)]$ with Mo–Ge = 2.658(2) Å,⁵⁴ and the tungsten complexes $[(\eta^5\text{-C}_5\text{Me}_5)\text{W}(\text{CO})(\text{EtNC})(\text{PMe}_3)(\text{GeCl}_3)]$ with W–Ge = 2.493(2) Å,⁵⁵ $[(\eta^5\text{-C}_5\text{Me}_5)\text{W}(\text{CO})_2\{\text{C}(\text{H})\text{NEt}_2\}(\text{GeCl}_3)]$ with W–Ge = 2.5269(9) Å,⁵⁵ $[(\eta^5\text{-C}_5\text{H}_5)\text{W}(\text{SiMe}_3)(\text{GeMe}_2\text{Cl})]$ with W–Ge = 2.542(1) Å,⁵⁶ and *cis*- $[(\eta^5\text{-C}_5\text{Me}_5)\text{W}(\text{CO})_2(\text{PMe}_3)(\text{GeCl}_3)]$ with W–Ge = 2.5590(5) Å,⁵⁷ and **12** with W–Ge = 2.681(3) Å.¹³

(49) Wells, A. F. *Structural Inorganic Chemistry*, 5th ed.; Clarendon: Oxford, 1984; pp 1279 and 1288. Pauling, L. *The Nature of the Chemical Bond*, 3rd ed.; Cornell University Press: Ithaca, NY, 1960; p 256.

(50) Pauling, L. *The Nature of the Chemical Bond*, 3rd ed.; Cornell University Press: Ithaca, NY, 1960; p 239: The relationship of bond order to bond distance is given by $d_n = d_1 - 0.71 \log(n)$, where n is the bond order, d_1 and d_n are the bond distances with bond order 1 and n , respectively. The value of n for the M≡Ge bond is 3.05 in **1a**, 2.95 in **1b**, 2.98 in **1c** and **1d**, and 2.93 in **1e**.

(51) Filippou, A. C.; Winter, J. G.; Kociok-Köhn, G.; Hinz, I. *J. Organomet. Chem.* **1997**, *542*, 35.

(52) Filippou, A. C.; Winter, J. G.; Kociok-Köhn, G.; Hinz, I. *J. Organomet. Chem.* **1997**, *544*, 225.

(53) Carré, F.; Colomer, E.; Corriu, R. J. P.; Vioux, A. *Organometallics* **1984**, *3*, 970.

(54) Chan, L. Y. Y.; Dean, W. K.; Graham, W. A. G. *Inorg. Chem.* **1977**, *16*, 1067.

(55) Filippou, A. C.; Portius, P.; Winter, J. G.; Kociok-Köhn, G. *J. Organomet. Chem.* **2001**, *628*, 11.

(56) Figge, L. K.; Carroll, P. J.; Berry, D. H. *Organometallics* **1996**, *15*, 209.

(57) Filippou, A. C.; Winter, J. G.; Feist, M.; Kociok-Köhn, G.; Hinz, I. *Polyhedron* **1998**, *17*, 1103.

Table 2. Selected Optimized Geometrical Parameters of the Metallogermylenes $[(\eta^5\text{-C}_5\text{H}_5)(\text{CO})_3\text{M}-\text{GeMe}]$ ($\text{M} = \text{Cr}, \text{Mo}, \text{W}$) and $[(\eta^5\text{-C}_5\text{H}_5)(\text{CO})_2\text{Fe}-\text{GeMe}]$, and X-ray Data of **11** and **12**^{a,b}

	M = Cr (Ia)			M = Mo (Ib)		M = W (Ic)			M = Fe (IId)	
	B3LYP	BP86	X-ray (11)	B3LYP	BP86	B3LYP	BP86	X-ray (12)	B3LYP	BP86
Bond Distances										
M–Ge	2.647	2.615	2.590(2)	2.716	2.695	2.752	2.697	2.681(3)	2.436	2.404
M–CO ^c	1.843	1.839	1.833(10)	1.993	1.978	1.983	1.978	2.00(2)	1.752	1.742
	1.839	1.831	1.889(16)	1.999	1.979	1.992	1.980	1.99(2)		
M–C(Cp)av	2.244	2.238	2.13(2)	2.425	2.401	2.411	2.400	2.35(2)	2.154	2.138
Ge–CH ₃	2.024	2.022	1.989(8)	2.014	2.018	2.021	2.018	1.99(2)	2.035	2.037
C–O ^c	1.166	1.171	1.151(6)	1.156	1.170	1.168	1.171	1.17(2)	1.159	1.165
	1.158	1.163	1.153(10)	1.148	1.163	1.160	1.164	1.18(2)		
Bond Angles										
M–Ge–CH ₃	107.1	108.0	117.8(2)	109.8	110.1	108.3	110.0	114.7(6)	107.8	107.6
Ge–M–CO ^d	68.4	68.0		69.0	69.2	69.6	69.3	75.4(6)	85.2	85.8
								71.8(6)		
Ge–M–CO ^e	127.4	126.9		129.5	129.4	130.1	129.4	134.8(7)		
C(O)–M–C(O)	110.2	108.0	102.4(5)	103.5	102.1	103.5	102.1	102.2(9)	94.1	92.7

^a Distances are in Å, and angles are in degrees. ^b X-ray data are taken from ref 13. ^c The first value refers to the CO groups which are syn to Ge; the second value refers to the trans CO ligand. ^d CO is syn to Ge. ^e CO is anti to Ge.

The Ge–C optimized bond distances 1.981 Å in **Ia**, 1.979 Å in **Ib**, 1.975 Å in **Ic**, and 1.982 Å in **IId** are as expected for a single bond based on covalent radii predictions (Ge–C = 1.99 Å). Only the cationic iron complex, **Ie**, possesses a Ge–C distance which is about 0.06 Å shorter as compared to **Ia–Id**. The M–Ge–C bond angles in **Ia–Id** deviate slightly from linearity.

Metallogermylenes $[(\eta^5\text{-C}_5\text{H}_5)(\text{CO})_3\text{M}-\text{GeMe}]$ (**Ia**, $\text{M} = \text{Cr}$; **Ib**, $\text{M} = \text{Mo}$; **Ic**, $\text{M} = \text{W}$) and $[(\eta^5\text{-C}_5\text{H}_5)(\text{CO})_2\text{Fe}-\text{GeMe}]$, **IId**. Figure 3 shows the optimized geometries of the metallogermylenes **Ia–IId**. The theoretical bond lengths and angles computed using the B3LYP and the BP86 exchange-correlation functionals are presented in Table 2. Both levels of theory B3LYP and BP86 give optimized geometries which are in good agreement with experimental results of $[(\eta^5\text{-C}_5\text{H}_5)(\text{CO})_3\text{M}-\text{GeR}]$ (**11**, $\text{M} = \text{Cr}$; **12**, $\text{M} = \text{W}$). The molybdenum complex $[(\eta^5\text{-C}_5\text{H}_5)(\text{CO})_3\text{Mo}-\text{GeR}]$ has not been isolated so far. There are no X-ray structural data for the iron complex **IId** known to us. We report here for the first time a structure of a ferroggermylene complex. The bent geometries at germanium (M–Ge–C3 bond angles: 108.0° in **Ia**, 110.1° in **Ib**, 110.0 in **Ic**, and 107.6 in **IId**) in these complexes are consistent with the presence of a divalent germanium(II) center, which is singly bonded to a transition metal and carbon. The metal–germanium bond distances 2.615 Å in **Ia**, 2.695 Å in **Ib**, and 2.697 Å in **Ic** are longer than those expected for a single bond based on covalent radii predictions (Cr–Ge = 2.50 Å, Mo–Ge = 2.62 Å, and W–Ge = 2.63 Å).⁴⁹ However, the Fe–Ge bond distance 2.404 Å in **IId**, which is the shortest M–Ge bond distance of a metallogermylene in this study, is shorter than the sum of the covalent radii of iron and germanium (Fe–Ge = 2.48 Å). The calculated Ge–C bond distances 2.022 Å in **Ia**, 2.018 Å in **Ib**, 2.018 Å in **Ic**, and 2.037 Å are longer than those found in the metal germylyne complexes (Table 1). For the known σ bonded monomeric alkyl or aryl germylenes, the Ge–C bond lengths range between 1.99 and 2.08 Å, and the C–Ge–C angle varies from 98° to 108.4°.^{26–30} The Ge–C bond distances and M–Ge–C bond angles in metallogermylene complexes are within the range of mononuclear nonmetallic germylenes.^{17–24} Hence, the calculated geometries of the compounds **Ia–IId** agree with those of known structures of germylenes with one metal fragment as a substituent.

Table 3. Wiberg Bond Indices (WBI) of the Metal Germylyne Complexes **Ia–Ie** and Metallogermylenes **Ia–IId**

	WBI		
	M–Ge	Ge–CH ₃	M–CO
$[(\eta^5\text{-C}_5\text{H}_5)(\text{CO})_2\text{Cr}=\text{GeMe}]$ (Ia)	1.41	0.77	0.99
$[(\eta^5\text{-C}_5\text{H}_5)(\text{CO})_2\text{Mo}=\text{GeMe}]$ (Ib)	1.46	0.81	1.10
$[(\eta^5\text{-C}_5\text{H}_5)(\text{CO})_2\text{W}=\text{GeMe}]$ (Ic)	1.57	0.84	1.14
$[(\eta^5\text{-C}_5\text{H}_5)(\text{CO})\text{Fe}=\text{GeMe}]$ (Ie)	1.30	0.78	0.92
$[(\eta^5\text{-C}_5\text{H}_5)(\text{CO})_2\text{Fe}=\text{GeMe}]^{2+}$ (Ie)	0.78	0.83	0.65
$[(\eta^5\text{-C}_5\text{H}_5)(\text{CO})_3\text{Cr}-\text{GeMe}]$ (Ia)	0.42	0.80	0.95
			0.90
$[(\eta^5\text{-C}_5\text{H}_5)(\text{CO})_3\text{Mo}-\text{GeMe}]$ (Ib)	0.50	0.80	1.05
			0.99
$[(\eta^5\text{-C}_5\text{H}_5)(\text{CO})_3\text{W}-\text{GeMe}]$ (Ic)	0.53	0.80	1.11
			1.04
$[(\eta^5\text{-C}_5\text{H}_5)(\text{CO})_2\text{Fe}-\text{GeMe}]$ (IId)	0.58	0.78	0.88

Bonding Analysis of M≡GeMe and M–GeMe Bonds. We begin the analysis of the bonding situation in the germylyne complexes **Ia–Ie** and the metallogermylenes **Ia–IId** with a discussion of the conventional indices which are frequently used to characterize the bonding situation in molecules, that is, bond orders and atomic charges. Table 3 gives the Wiberg bond indices (WBI)⁵⁸ and the natural bond orbital (NBO)⁴⁵ charge distribution. To examine the charge flow between the GeMe⁺ ligand and the [M]^q metal fragments in the molecules, we calculated the atomic charges of the fragments in the frozen geometries of the molecules. The results are shown in Figure 4.

Table 3 shows that the WBI values of the M–Ge bonds of the neutral germylyne complexes **Ia–Id** are significantly higher (1.30–1.57) than the WBI values of the metallogermylenes **Ia–IId** (0.42–0.50). This is a first indication that the former molecules have a substantial degree of multiple M–Ge bonding. We want to point out that the germylyne complexes of the group-6 metals **Ia–Ic** have WBI values that are 3 times as high as those in the corresponding group-6 metallogermylenes **Ia–Ic** (Table 3). The WBI value of the double positively charged germylyne complex **Ie** (0.78), however, is much smaller than the data of the neutral species **Ia–Id**. The bond indices of the Ge–CH₃ and M–CO bonds of the two classes of compounds are not very different from each other.

(58) Wiberg, K. A. *Tetrahedron* **1968**, *24*, 1083.

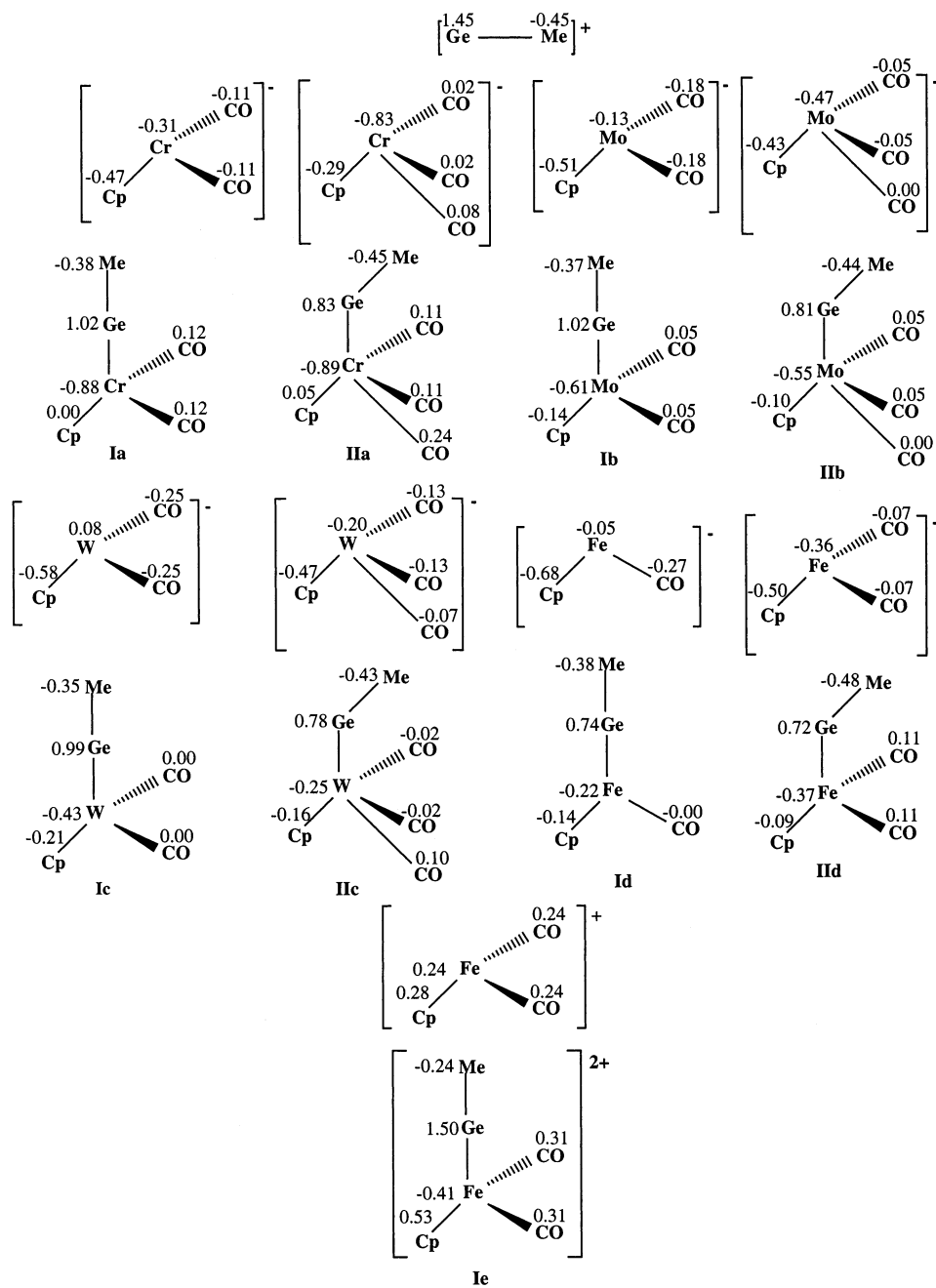


Figure 4. Calculated NBO partial charges of the neutral complexes **Ia–Id**, **IIa–IIId**, and the fragments $[\text{M}]^-$ and GeMe^+ .

The calculated charge distribution indicates that the metal atoms always carry a negative charge while the Ge atom and the GeMe ligand are positively charged. The neutral gerymylene complexes **Ia–Id** and the metallogerymylenes **IIa–IIId** exhibit interesting differences in the charge distribution. The GeMe ligand in the former compounds is more positively charged than that in the latter species. More information is revealed when the charge flows between the interacting fragments GeMe^+ and $[\text{M}]^q$ are compared. Figure 4 shows that the metal atoms of the gerymylene complexes $[(\eta^5\text{-C}_5\text{H}_5)(\text{CO})_n\text{M}\equiv\text{GeMe}]$ (**Ia–Id**) have a much higher negative charge than those in the respective fragments $[(\eta^5\text{-C}_5\text{H}_5)(\text{CO})_n\text{M}]^-$. This is remarkable, because there is an overall charge flow in the direction $[(\eta^5\text{-C}_5\text{H}_5)(\text{CO})_n\text{M}]^- \rightarrow \text{GeMe}^+$. It follows that the ligands Cp and CO donate electronic charge to the metal atom and to the gerymylene

ligand in **Ia–Id**. However, the metal atoms of the metallogerymylenes $[(\eta^5\text{-C}_5\text{H}_5)(\text{CO})_{n+1}\text{M}-\text{GeMe}]$ (**IIa–IIId**) have nearly the same charge as in the respective fragments $[(\eta^5\text{-C}_5\text{H}_5)(\text{CO})_{n+1}\text{M}]^-$, although the charge $[(\eta^5\text{-C}_5\text{H}_5)(\text{CO})_{n+1}\text{M}]^- \rightarrow \text{GeMe}^+$ is larger than in **Ia–Id** (Figure 4). It follows that the *change* in the charge distribution upon M–Ge bond formation but not the final charge distribution indicates a substantially different bonding situation between gerymylene complexes and metallogerymylenes. To quantify this information and to get a more detailed insight into the nature of the M–Ge interactions, we carried out an energy partitioning analysis. The results are given in Table 4.

The data in Table 4 show that the interaction energies of the neutral group-6 gerymylene complexes **Ia–Id** (–206.2 to –220.6 kcal/mol) are rather high. The contributions of the electrostatic

Table 4. Results of the Energy Decomposition Analysis of the Metal Germylyne Complexes $[(\eta^5\text{-C}_5\text{H}_5)(\text{CO})_2\text{M}\equiv\text{GeMe}]$ (**Ia**, M = Cr; **Ib**, M = Mo; **Ic**, M = W), $[(\eta^5\text{-C}_5\text{H}_5)(\text{CO})\text{Fe}\equiv\text{GeMe}]$, **Id**, $[(\eta^5\text{-C}_5\text{H}_5)(\text{CO})_2\text{Fe}\equiv\text{GeMe}]^{2+}$, **Ie**, and Metallogermylenes $[(\eta^5\text{-C}_5\text{H}_5)(\text{CO})_3\text{M}-\text{GeMe}]$ (**IIa**, M = Cr; **IIb**, M = Mo; **IIc**, M = W) and $[(\eta^5\text{-C}_5\text{H}_5)(\text{CO})_2\text{Fe}-\text{GeMe}]$, **IId**, at BP86/TZ2P^a

	Ia	Ib	Ic	Id	Ie	IIa	IIb	IIc	IId
ΔE_{int}	-206.2	-210.5	-220.6	-219.6	16.0	-165.1	-165.6	-168.1	-188.5
ΔE_{Pauli}	107.9	107.7	115.9	114.0	92.0	138.2	137.5	147.2	164.2
ΔE_{elstat}	-157.8	-160.8	-168.9	-172.3	34.1	-178.2	-174.7	-181.9	-209.7
ΔE_{orb}^b	-156.3	-157.4	-167.5	-161.4	-110.1	-125.2	-128.5	-133.4	-143.0
	(49.8%)	(49.5%)	(49.8%)	(48.4%)	(100%)	(41.3%)	(42.4%)	(42.3%)	(40.5%)
$\Delta E_{\sigma}(\sigma')$	-89.7	-90.7	-97.0	-74.6	-79.3	-99.6	-103.6	-107.7	-117.3
$\Delta E_{\pi}(\pi'')$	-66.6	-66.7	-70.5	-86.7	-30.8	-25.6	-24.9	-25.7	-25.7
	(42.6%)	(42.4%)	(42.1%)	(53.8%)	(28.0%)	(20.4%)	(19.3%)	(19.2%)	(18.0%)
ΔE_{prep}	5.2	5.8	7.4	0.8	3.3	13.5	12.3	12.4	11.9
$\Delta E(-D_e)$	-201.0	-204.7	-213.2	-233.0	19.3	-151.6	-153.3	-155.7	-176.6

^a Energy contributions in kcal/mol. ^b The values in parentheses are the percentage contribution to the total attractive interactions reflecting the covalent character of the bond. ^c The values in parentheses are the percentage contribution to the total orbital interactions, ΔE_{orb} .

attraction ΔE_{elstat} and the covalent bonding ΔE_{orb} have nearly the same value; that is, the $[\text{M}]^- - \text{GeMe}^+$ bonding in **Ia–Id** is half covalent and half electrostatic. The covalent bonding has a high degree of π character. We want to emphasize that the calculated energy contribution ΔE_{π} gives only the out-of-plane (π_{\perp}) component of the $[\text{M}]^- \rightarrow \text{GeMe}^+$ π back-donation, which is schematically shown in Figure 1a. This is because the molecules have C_s symmetry, and thus the orbitals can only have $a'(\sigma)$ or $a''(\pi)$ symmetry. Thus, the energy contributions of the $a'(\sigma)$ orbitals come from the $[\text{M}]^- \leftarrow \text{GeMe}^+$ σ donation but also from the in-plane $[\text{M}]^- \rightarrow \text{GeMe}^+$ back-donation. For molecules which have only C_s symmetry, it is not possible to separate the latter two interactions because the orbitals have a' symmetry. An energy partitioning analysis of the germylyne complex $[\text{Cl}(\text{CO})_4\text{W}\equiv\text{GeH}]$, which has C_{4v} symmetry, showed that the total contribution of the $[\text{M}]^- \rightarrow \text{GeH}^+$ π back-donation is 78.0% of ΔE_{orb} .^{59,60}

The energy analysis suggests that, in **Ia–Ic**, ~42% of the ΔE_{orb} term comes from $(a'')\pi$ bonding. It is remarkable that the relative contributions of the different energy terms in Cr, Mo, and W complexes are nearly identical. The neutral iron germylyne complex **Id** has a higher degree of $(a'')\pi$ bonding (53.8%), but the relative contributions of ΔE_{elstat} , ΔE_{Pauli} , and ΔE_{orb} to the interaction energy are not very different from the data of the group-6 complexes **Ia–Ic**. The doubly charged iron complex **Ie** is predicted to have a repulsive interaction energy with respect to the fragments $[\text{Fe}]^+$ and GeMe^+ (Table 4). The electrostatic interactions are repulsive, and the only attractive term is ΔE_{orb} which has 28.0% $(a'')\pi$ character. Thus, **Ie** is held together like many other dications by covalent bonding, which prevents the Coulomb explosion of the molecule.⁶¹

What is the difference between the energy contributions of **Ia–Id** and **IIa–IId**? First, the total interaction energies ΔE_{int} in the metallogermylenes **IIa–IId** are less attractive than those in the germylyne complexes **Ia–Id**. The differences are between 41.1 (**IIa–Ia**) and 52.5 kcal/mol (**IIc–Ic**). The metallogermylenes **IIa–IId** have a slightly lower degree of covalent bonding (40.5%–42.4%) than the germylyne complexes **Ia–Id** (48.4%–49.8%). However, the largest differences between the two classes of compounds are found for the degree of $a''(\pi)$ bonding. The contribution of ΔE_{π} to the covalent term ΔE_{orb} is

much higher in **Ia–Id** (42.1%–42.6% in the group-6 species **Ia–Ic** and even 53.8% in **Id**) than in **IIa–IId** (18.0%–20.4%). This shows that the $a''(\pi)$ contributions to the $[\text{M}]^- - \text{GeMe}^+$ bonding in the metallogermylenes are much weaker than the out-of-plane π contributions in the germylyne complexes. This can be explained with the much longer M–Ge bond lengths in the former compounds than in the latter. Another factor which contributes to the weaker $a''(\pi)$ bonding in **IIa–IId** is that the $[\text{M}]^- \rightarrow \text{GeMe}^+$ π back-donation competes with the π acceptor strength of three CO ligands (two in **IId**), while there are only two CO ligands in **Ia–Ic** (one in **Id**). While the π bonding contributions in **IIa–IId** are weaker than those in **Ia–Id**, the σ bonding contributions in the former compounds are stronger than those in the latter. Note that not only the relative (%) values but also the absolute values of ΔE_{σ} in **IIa–IId** are larger than those in **Ia–Id** (Table 4). The finding that the $\sigma(a')$ interactions in complexes **II** are more important than in **I** is surprising. It may be explained with the different hybridization of the germanium atom in the metallogermylenes and germylyne complexes. This will be shown below.

To visualize the differences in the M–Ge bonding between the metal-germylyne complexes and the metallogermylenes, envelope plots of some relevant orbitals of the tungsten-germylyne complex $[(\eta^5\text{-C}_5\text{H}_5)(\text{CO})_2\text{W}\equiv\text{GeMe}]$ **Ic** and the tungsten-germylyne compound $[(\eta^5\text{-C}_5\text{H}_5)(\text{CO})_3\text{W}-\text{GeMe}]$ **IIc** are shown in Figure 5. Figure 5a (HOMO-1) and 5b (HOMO-2) gives a pictorial description of the W–Ge π bonding in the complex **Ic**. The HOMO-1 is a true π orbital; that is, it has $a''(\pi)$ symmetry. The HOMO-2 has a' symmetry, and thus it is a σ orbital. However, the shape of the orbital shows nicely that the HOMO-2 can be identified with the π_{\parallel} component of the π back-donation (Figure 1a). The HOMO of **IIc** (Figure 5c) is mainly the lone-pair orbital at Ge, which has, however, some in-plane pseudo π bonding contributions. The HOMO-3 of **IIc** (Figure 5d) shows mainly the Ge–W σ bonding orbital. The actual HOMO and HOMO-3 orbitals of **IIc** may be compared with the σ bonding components of the qualitative orbital model, which is given in Figure 1c. It becomes obvious that the hybridization at the M–GeR moiety is different from the qualitative model, but the difference in the bonding situation between **Ic** and **IIc** which is sketched in Figure 1a and 1c is nicely recovered in the shape of the orbitals, which are shown in Figure 5. It becomes clear that the former species has a large contribution from π bonding orbitals, while **IIc** is a σ bonded species. Note that there are two $\sigma(a')$ bonding orbitals in the

(59) Lein, M. Diploma Thesis; Marburg, 2001.

(60) Lein, M.; Szabo, A.; Kovacs, A.; Frenking, G. *Faraday Soc. Discuss.*, in print.

(61) Koch, W.; Frenking, G. *Chem. Phys. Lett.* **1985**, *114*, 178.

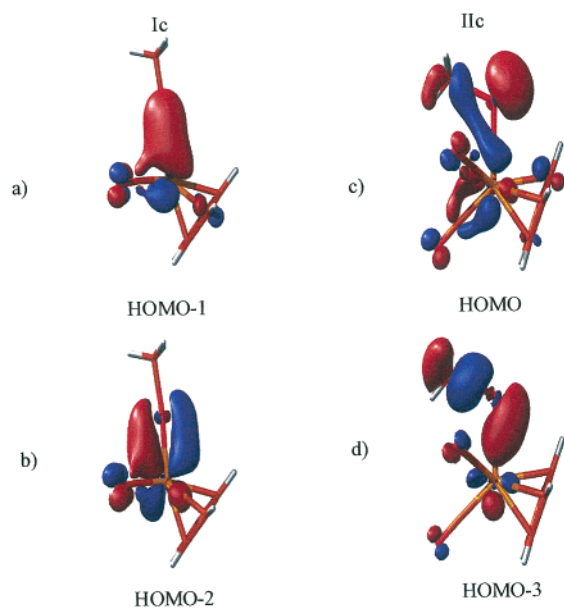


Figure 5. Plot of some relevant orbitals of **Ic** and **IIc**.

latter compound but only one in **Ic**. This is an a posteriori explanation for the finding that the $\sigma(a')$ interactions in complexes **II** are more important than those in **I**.

Summary and Conclusion

We have presented the first theoretical study where the bonding situations in germylyne complexes and metallogermylenes are compared with each other. The calculated geometries are in excellent agreement with experimental values.

The analysis of the electronic structure of the neutral metal germylyne complexes **Ia–Id** and the metallogermylenes **IIa–IIId** shows that the former compounds have about the same degree of electrostatic and covalent bonding, while the relative strength of the covalent contributions in the latter molecules is lower (41–42%) than the electrostatic attraction (58–59%). The $a''(\pi)$ bonding contributions in the group-6 germylyne complexes **Ia–Ic** are rather high (42% of the orbital interactions in **Ia–Ic** and 53.8% in **Id**). The π bonding contributions to the covalent bonding become much less (18–20%) in the metallogermylenes **IIa–IIId**. The calculations show clearly that there are two classes of compounds which have a M–Ge–R linkage, that is, Fischer-type metal germylyne complexes **I** and metallogermylenes **II**. The second class of compounds is not known for transition metal complexes with carbyne ligands CR, while analogous Schrock-type carbyne complexes¹⁰ (metal alkylidyne) are not yet known for [M]GeR compounds.

Acknowledgment. This work was supported by the Deutsche Forschungsgemeinschaft and by the Fonds der Chemischen Industrie. K.K.P. thanks the Alexander von Humboldt Foundation for a research fellowship. Excellent service by the Hochschulrechenzentrum of the Philipps-Universität Marburg is gratefully acknowledged. Additional computer time was provided by the HLRS Stuttgart and HHLRZ Darmstadt.

Supporting Information Available: Tables with the Cartesian coordinates of the optimized geometries of **Ia–IIId** (PDF). This material is available free of charge via the Internet at <http://pubs.acs.org>.

JA020974M